International Journal of MATERIALS RESEARCH Zeitschrift für METALLKUNDE Original Contributions

T. Woehrle et al.: Fe-N and Fe-N-C phase equilibria above 853 K studied by nitriding/nitrocarburising

Thomas Woehrle^a, Havva Cinaroglu^b, Andreas Leineweber^{a,c}, Eric Jan Mittemeijer^{a,b}

- ^aMax Planck Institute for Intelligent Systems (formerly Max Planck Institute for Metals Research), Stuttgart, Germany
- ^bInstitute for Materials Science, University of Stuttgart, Stuttgart, Germany
- ^c Institute of Materials Science, TU Bergakademie Freiberg, Freiberg, Germany

Fe–N and Fe–N–C phase equilibria above 853 K studied by nitriding/nitrocarburising and secondary annealing

Compound-layer microstructures obtained by gaseous nitriding and nitrocarburising treatments of α-Fe and Fe-N alloy and by subsequent treatments were analysed to obtain new information on the metastable Fe-N and Fe-N-C systems above 853 K at 1 atm. In the case of the binary Fe-N system, invariant temperatures and phase boundaries agree well with the literature data, only the $\gamma/\gamma + \gamma'$ and the γ/γ $\gamma + \varepsilon$ boundaries as determined in the present work by means of electron probe microanalysis are located at N contents up to 1 at.% lower than reported in previous works. In the case of the ternary Fe-N-C system, the invariant eutectoid reaction was found to occur in the range 853 K-863 K, whereas the invariant transition reaction was found to occur in the range 868 K-873 K. The obtained data were used to draw isothermal sections of the Fe-N-C system for 853 K and 893 K. The determined temperatures for the invariant eutectoid and transition reactions as well as the extent of the ternary ϵ -phase field were compared with phase diagrams calculated on the basis of different thermodynamic descriptions of the Fe–N–C system.

Keywords: Phase diagram; Phase equilibria; Interstitial phases; Iron carbonitrides

1. Introduction

The use of diffusion couples [1-5] is a powerful experimental method to determine phase equilibria and phase-

boundary concentrations in a multicomponent system. Thereby, two different phases are brought into direct contact and annealed at a temperature high enough to realise distinct atomic mobility. During annealing, reactive diffusion can lead to formation of one or more new phases between the initial end members of the diffusion couple. Thereby, the evolution of the average composition as a function of "depth", i.e. in a direction perpendicular to the original interface of the diffusion couple [1-3], yields the diffusion path. That diffusion path can be taken as the evolution with depth of the n (average) molar fractions of the n components of the system through the n-dimensional space spanned by these n molar fractions. If local equilibrium prevails everywhere at the solid-solid interphase boundaries in the diffusion zone, the sequence of the phases developing within the diffusion zone and the diffusion path can be related with the corresponding phase diagram [1-3]. At a given temperature and pressure, the course of a diffusion path is governed by both thermodynamics (e.g. the possible phase equilibria) and kinetics (e.g. the mobility of each component in a system).

Note, however, that it is well possible that the velocity of the phase interfaces is not solely controlled by diffusion as can be the case if local equilibrium is realized. In such cases deviations from local equilibrium can occur [6]. Care has to be taken to identify microstructures for which this is the case, e.g. in the case that not all microstructures can be reconciled with the same phase diagram under assumption of local equilibrium at all phase interfaces. As a consequence one has to arrive at some kind of most likely phase diagram in view of the experimental evidence available.

Solid-state phase equilibria in the metastable binary Fe-N and the metastable ternary Fe–N–C systems¹ are of great importance, in particular for the widely applied nitriding and nitrocarburising processes, where nitrogen and/or carbon diffuse into the surface of iron or iron-based alloys, usually at temperatures between 823 K and 853 K [7-9]. If the chemical potential of nitrogen and/or carbon as pertaining to the nitriding/nitrocarburising medium is sufficiently high, a compound layer develops at the surface of the workpiece, which is typically composed of the iron(carbo)nitrides ε -Fe₃(N,C)_{1+x} and γ' -Fe₄N_{1-z} [8, 10–14]. Upon nitrocarburising under certain conditions θ-Fe₃C can also be formed in the compound layer [15-17]. The compound layers can lead to a significant improvement of the mechanical (resistance to wear and friction) and chemical (resistance to corrosion) properties of the workpiece [18–20].

Up to now, fundamental research on the Fe–N and Fe–N–C systems has involved extensive experimental work on the nitriding and nitrocarburising of iron powders and iron foils. These works have cumulated in purely experimental versions of the phase diagrams Fe–N [21, 22] and Fe–N–C [23–25], all pertaining to 1 atm. Such experimental data have been used to obtain corresponding thermodynamic descriptions of the Fe–N [26–31] and Fe–N–C systems [29, 32–37] allowing for calculation of the phase equilibria by using the Calphad method.

Especially the ternary Fe–N–C phase diagrams calculated on the basis of different thermodynamic descriptions differ considerably with respect to the phase boundaries and temperatures of the invariant reactions found experimentally. This is especially evident in the technologically crucial temperature range of 773 K–873 K and slightly above, within which several invariant reactions occur. In view of these discrepancies it is necessary to improve the amount and also the quality of the experimental information on the constitution of the Fe–N–C system.

A striking example of such a knowledge gap (and controversy in the literature) concerns the minimum temperatures at which the $\alpha + \epsilon$ two-phase field may occur in the ternary Fe–N–C system, and whether it exists at all (it does not exist in the binary Fe–C and Fe–N systems). Novel experimental data suggested that this $\alpha + \epsilon$ two-phase field forms above a temperature between 833 K and 843 K by a transition type invariant reaction from a θ (cementite) + γ' two-phase field, which occurs at lower temperatures [38]. The latter work is one example of our activities to re-investigate some of the important phase equilibria in the Fe–N–C system [13, 14, 39, 40]. The approach followed in these studies was based on:

a. Systematic analysis of phase microstructure and composition in the compound layers generated by nitrocarburising. Here the *diffusion path* in a compound layer can be given by the evolution of the laterally averaged molar fractions of N and C (that of Fe follows from these as all molar fractions add up to 1) with depth (= distance from surface). If local equilibrium prevails the diffusion path and the correspondingly observed phases can be re-

- lated to the occurrence of two-phase, three-phase and at most four-phase (invariant at constant pressure) equilibria in the Fe–N–C phase diagram at the temperature of the nitrocarburising treatment [40].
- b. Nitrocarburising *N-presaturated* α -iron substrates. These substrates expose the difficulty of establishing certain solid-state equilibria upon nitrocarburising *N-free* (pure) α -iron substrates [40] due to initial formation of cementite layers acting as a diffusion barrier for nitrogen [41].
- c. So-called secondary anneals under inert atmosphere applied to specimens previously nitrocarburised at temperatures identical to or different from the annealing temperature [38, 39, 42]. Such anneals can level out concentration gradients and, because of this and/or an annealing temperature different from the nitrocarburising temperature, may induce new phase transformations in the compound layer. Analysis of the resulting microstructures can give insight into the presence of phase equilibria at the temperature of the secondary anneal.

Using the above-described experimental methods, the present paper focusses on the solid-state equilibria in the Fe–N and Fe–N–C systems above 853 K.

2. Experimental

2.1. Specimen preparation; nitriding and nitrocarburising experiments

Rectangular specimens of dimensions $20 \times 25 \times 1 \text{ mm}^3$ were cut from cold-rolled cast iron plates (Alfa Aesar, 99.98 wt.%), ground, polished (final stage 1 µm diamond suspension), cleaned ultrasonically in ethanol and recrystallised in hydrogen for 2 h at 973 K. Directly before nitriding or nitrocarburising the specimens were polished (final stage 1 µm diamond suspension) and cleaned with ethanol.

Several series of gaseous nitriding and gaseous nitrocarburising experiments were performed in a vertical fused-silica tube furnace of 28 mm diameter. The pure nitriding experiments were carried out in gas mixtures containing NH₃, H_2 and sometimes additionally N_2 . The nitrocarburising experiments were carried out in gas mixtures containing NH₃, H_2 , CO and sometimes additionally CO_2 , N_2 and H_2O . The process temperature was controlled within ±1 K in the middle of the furnace, where the specimen was placed suspended on a fused-silica fibre. The composition of the gas atmosphere was adjusted by separate mass-flow controllers for NH₃ as nitriding species, CO and CO₂ as carburising species, N2 as inert gas, H2 as well as (deionized) evaporated H₂O (all gases from Westfalen AG with a purity of 99.999 vol.% except CO with a purity of 99.997 vol.%). Significant dissociation of NH₃ and the occurrence of side reactions in the gas atmosphere, which both would affect the composition of the gas mixture, were minimised by application of a high overall linear gas-flow rate through the fused-silica tube of 13.5 mm s⁻¹ as calculated for the gas volume at room temperature. Upon nitrocarburising the gas-supply lines were heated to 393 K to avoid the condensation of ammonium bicarbonate. After the heat treatment the specimens were quenched in water (flushed with nitrogen) at room temperature.

Pure nitriding experiments (series N) were conducted to investigate the solid state phase equilibria and phase trans-

¹ The intermediate solid phases in the binary Fe–N and the ternary Fe–N–C system are metastable with respect to the decomposition into iron, nitrogen and/or carbon. All equilibria considered here refer to the metastable equilibria.

formations in the binary Fe–N system at temperatures between 873 K and 993 K (see Table 1); i.e. above the temperature of the eutectoid $\gamma \rightleftharpoons \alpha + \gamma'$ at 865 K [21, 43]. The composition of the nitriding atmosphere was chosen such that the ϵ phase with a nitrogen content >20 at.% is obtained at the surface of the compound layer in equilibrium with the gas atmosphere [44]; see Table 1.

Nitrocarburising of pure α -iron substrates (series NC863) and nitrogen pre-saturated α -iron substrates (series NC) were performed to investigate the phase transformations in the ternary Fe–N–C system in the temperature range of 853 K–893 K. The process parameters are given in Table 2 and Table 3, respectively. The nitrogen pre-saturated substrates were obtained by nitriding of pure α -iron substrates $(20 \times 25 \times 1 \text{ mm}^3)$ for 64 h at 833 K in a gas mixture containing 10.9 vol.% NH₃ and 89.1 vol.% H₂. These nitriding conditions allow a maximum uptake of nitrogen in solid solution in the α -iron substrate without forming an iron-nitride compound layer [43, 45]. The absence of a compound layer was verified by X-ray diffraction.

The microstructure and composition of the compound layers obtained upon nitrocarburising of pure α -iron substrates at 853 K and 893 K were investigated as function of the carbon activity (at a given nitrogen activity) imposed by the gas mixture (series NC853 and NC893; see Table 2).

The gas atmospheres of the nitrocarburising experiments of series NC853, NC863, and NC893 were composed such that at the corresponding treatment temperature the two main carburising reactions, the Boudouard reaction and the heterogeneous water-gas reaction, are associated with the same chemical potential of carbon [46]. Therefore, for series NC853, NC863, and NC893 the nitrogen and carbon activities as calculated according to Ref. [46] have been indicated in Table 2. The (strongly) carburising character of the atmospheres for series NC was achieved by simply adding CO to NH₃, H₂ and N₂. Thereby, no definite value of the chemical potential of carbon is defined. It is theoretically infinite, if no side reactions changing the composition of the gas phase are considered [47]. Therefore, for simplicity only the value for the nitriding potential r_N and the volume fraction of CO have been listed in Table 3. It has to be emphasised that, anyway, in the present work only solid-state

Table 1. Nitriding experiments of series N: Process parameters, resulting compound-layers microstructures and maximum N content in the γ phase as determined by EPMA.

| Series | <i>T</i> (K) | $r_{\rm N}$ (atm ^{-1/2}) | Time (h) | layer | max. N content in γ (at.%) |
|--------|--------------|------------------------------------|----------|----------|----------------------------|
| N | 873 | 0.95 | 4 | ε/γ'/γ | 8.4 |
| | 893 | 0.80 | 4 | ε/γ'/γ | 8.6 |
| | 913 | 0.70 | 4 | ε/γ'/γ | 9.3 |
| | 923 | 0.60 | 4 | ε/γ'/γ | 9.3 |
| | 925 | 0.60 | 4 | ε/γ'/ε/γ | _ |
| | 928 | 0.60 | 4 | ε/γ'/ε/γ | _ |
| | 933 | 0.55 | 4 | ε/γ'/ε/γ | 9.3 |
| | 938 | 0.55 | 4 | ε/γ'/ε/γ | _ |
| | 948 | 0.50 | 4 | ε/γ | _ |
| | 953 | 0.50 | 4 | ε/γ | 9.2 |
| | 993 | 0.25 | 2 | ε/γ | 9.0 |

equilibria are considered. No conclusions are drawn which require the presence of an equilibrium or some stationary state [43] between the gas atmosphere and the surface of the solid.

Some nitrocarburized specimens were encapsulated in an evacuated fused-silica tube under an argon pressure of 0.3 atm and annealed in the nitriding/nitrocarburising furnace (see above) for 24 h. The annealing temperature was controlled within ±1 K. After annealing the specimens were quenched in water by destroying the fused-silica tube. The secondary annealing experiments were performed to (i) level off the nitrogen and carbon gradients in the compound layer as developed upon nitrocarburising and (ii) to approach (near) solid-state equilibria in the microstructure of the specimen (compound layer and substrate) at the annealing temperature.

2.2. Specimen characterisation

The nitrided/nitrocarburised specimens were cut into three pieces for optical microscopy, X-ray diffraction (XRD) and electron-probe microanalysis (EPMA), respectively.

Optical micrographs on cross-sections of the compound layers were taken using a Zeiss Axiophot microscope. For that the specimens were electroplated with a protective nickel layer using a Watts bath [10] at 333 K to prevent damaging and rounding of the compound layer close to the surface during sample preparation. Subsequently, the specimens were embedded (Polyfast, Struers GmbH), ground, polished (final stage: 1 µm diamond suspension) and etched in 1 vol.% Nital containing 0.1 vol.% HCl [48]. When needed, the compound layers obtained upon nitrocarburising were additionally stained with Groesbeck reagent [49] (4 g KMnO₄, 1 g NaOH, 1 g KOH per 100 ml H₂O) at

Table 2. Process parameters used for nitrocarburising of pure α -iron substrates (series NC863, NC853 and NC893).

| Series | T(K) | $a_{ m N}$ | $a_{\rm C}$ | NH ₃ (vol.%) | Time (h) |
|----------------|--------------------------|---------------------------------------|---------------------|----------------------------|-------------|
| NC853 NC863 | 853 853 863 863 | 553 ^a 415 ^b 109 | 0–500 0–500 2 | 16–20 16–20 12 | 4 4 4 |
| NC893 | 893 | 109 626 ^a | 0–200 | 12 18 | 4 4 |

^a Corresponds to conditions for which, in the case of pure nitriding, the ε phase would form [45].

Table 3. Process parameters and resulting compound-layer microstructures for nitrocarburising of nitrogen pre-saturated α -iron substrates (series NC).

| Series | T(K) | $r_{ m N}$ (atm ^{-1/2}) | CO (vol.%) | Time (h) | layer |
|--------|------|-----------------------------------|---------------|----------|-------|
| NC | 853 | 0.3 | 20 | 6 | θ/ε |
| | 868 | 0.3 | 20 | 6 | θ/ε |
| | 873 | 0.3 | 20 | 6 | θ/ε/γ |

^b Corresponds to conditions for which, in the case of pure nitriding, the γ' phase would form [45].

313 K, leading to an increased staining with increasing carbon content of a phase. Thereby, the γ' , ϵ , γ and cementite (θ) phases can be distinguished. Note that the γ phase formed at the treatment temperatures transforms partially into martensite (α') upon the quenching. Occurrence of this transformation is evident in the metallographic cross-sections and also in the XRD data. Since the presence of γ at the treatment temperature is relevant in the present context, γ or α' observed at room temperature is simply indicated as γ .

A compound layer can be divided into separate sublayers perpendicular to the surface normal, where each sublayer comprises a laterally homogeneous phase constitution, as observed over a lateral distance of at least several 10 µm. The overall phase constitution of the compound layer can thus be denoted [14, 40] by the sequence of phase compositions of the sublayers (separated by "/"), starting from the surface of the material and ending at the interface between compound layer and substrate. As opposed to pure nitride layers, the carbonitride layers resulting from nitrocarburising can contain sublayers containing two different phases, for which the Greek letters denoting the two phases are separated by a "+". The possibility of establishing two-phase sublayers upon nitrocarburising of pure iron is a consequence of Gibbs' phase rule for the case of three components (Fe, N, C) in the system.

The nitrogen and carbon contents in the compound layers were determined by EPMA on polished cross-sections of the specimens (final stage: 1 µm diamond suspension). For that purpose a Cameca SX100 microprobe equipped with five wavelength-dispersive spectrometers was used. Prior to the measurement, oxygen was blown for 40 seconds onto the cross-section at the position of the focused electron beam in order to remove carbon contamination from the sample surface. Line scans were performed with a step size of 1 µm at different locations of the compound layer perpendicular to the surface. The elemental concentrations were obtained from the simultaneously measured intensities of the characteristic N-K $_{\!\alpha},$ C-K $_{\!\alpha}$ and Fe-K $_{\!\alpha}$ radiations excited by an incident 10 keV-electron beam. The measured Ka intensities of N, C and Fe were compared with standard samples of α -Fe, γ' -Fe₄N₁₋₇ and θ Fe₃C. The concentrations of N, C and Fe were calculated from the intensity ratios applying the $\Phi(\rho z)$ approach [50]. The nitrogen and carbon contents at interphase boundaries were obtained by the extrapolation of the measured nitrogen concentration-depth profiles to these positions.

Phase analysis was performed by means of XRD using a PANalytical X'Pert Multi-Purpose Diffractometer equipped with a graphite monochromator in the diffracted beam (Co- K_{α} radiation) and applying Bragg–Brentano geometry. For better crystallite statistics the specimens were rotated around their surface normal during the measurement.

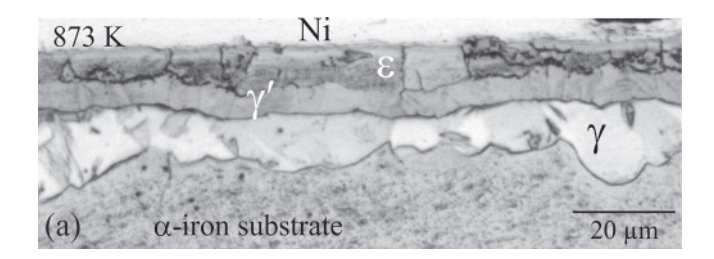
3. Results

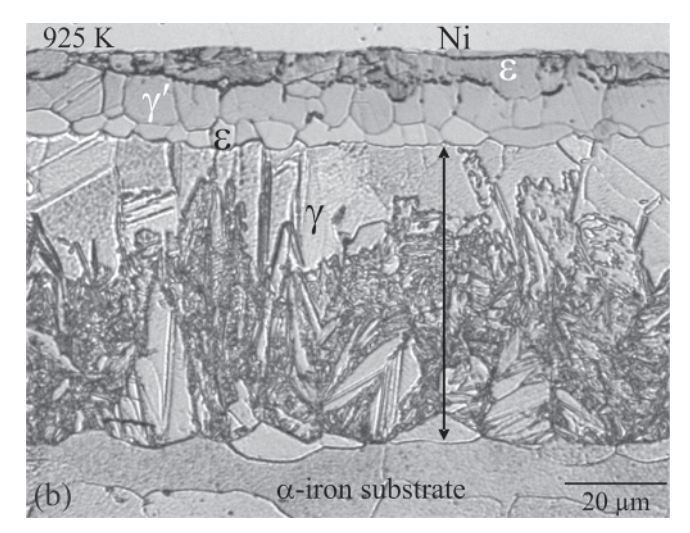
The following paragraphs report on the phase constitution in the compound layers as determined on the basis of optical micrographs recorded from cross-sections. In all cases, the results of XRD analysis of the compound layers was always well compatible with the results from optical microscopy. Hence, the diffraction results are not reported separately.

3.1. Nitriding experiments of Series N

Nitriding experiments of series N (Table 1) led to formation of an $\varepsilon/\gamma'/\gamma$ layer for temperatures between 873 K and 923 K, whereas for temperatures in the range of 925 K $\leq T \leq$ 938 K an $\varepsilon/\gamma'/\varepsilon/\gamma$ layer was obtained. The γ' phase did not occur in the compound layer at $T \geq$ 948 K and thus an ε/γ double layer was observed. These compound-layer microstructures are summarized in Table 1, typical microstructural images are shown in Fig. 1.

A nitrogen concentration—depth profile in the compound layer formed by nitriding experiments of series N is shown in Fig. 2. The phase-boundary concentrations are shown in Fig. 3 superimposed with the binary Fe–N phase diagram as drawn in Ref. [21] and experimental data from Refs.





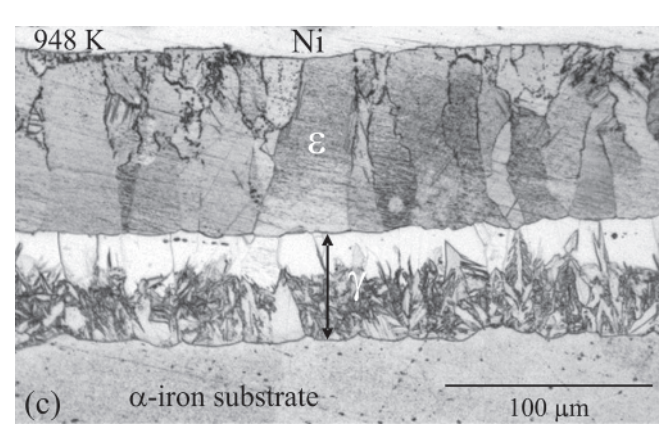


Fig. 1. Cross-sectional optical micrographs (after etching with 1 vol.% Nital containing 0.1 vol.% HCl) of the compound layers obtained upon nitriding of pure $\alpha\text{-iron}$ substrates for 4 h in NH $_3/\text{H}_2$ gas mixtures (series N) at (a) 873 K, (b) 925 K and (c) 948 K. For the case of the treatment temperatures of 925 K and 948 K, the extent of the γ sublayer is emphasised by an arrow.

[51–55] as cited in Ref. [21]. Since the N contents of the γ phase in equilibrium with the γ' or ϵ phases somewhat disagree with the earlier works, their values have additionally been listed in Table 1.

3.2. Nitrocarburising experiments of Series NC863 and NC

Nitrocarburising experiments of series NC863 conducted at 863 K (Table 2) resulted in the formation of a γ' layer ($a_{\rm C}$ = 2; Fig. 4a) and an ε + γ' / ε layer ($a_{\rm C}$ = 4; Fig. 4b). Additionally, in both cases, γ phase had developed at only some locations at the layer/substrate interface.

The nitrocarburising of nitrogen pre-saturated substrates with the same strongly carburising atmospheres but at different temperatures (series NC; Table 3) resulted in the formation of different microstructures, which all show a single-phase cementite (sub)layer at the surface of the substrate; see Fig. 5. A laterally homogeneous θ/ϵ double layer was obtained at 853 K. Such a θ/ϵ double layer was also obtained at 868 K, whereby some locations showed a

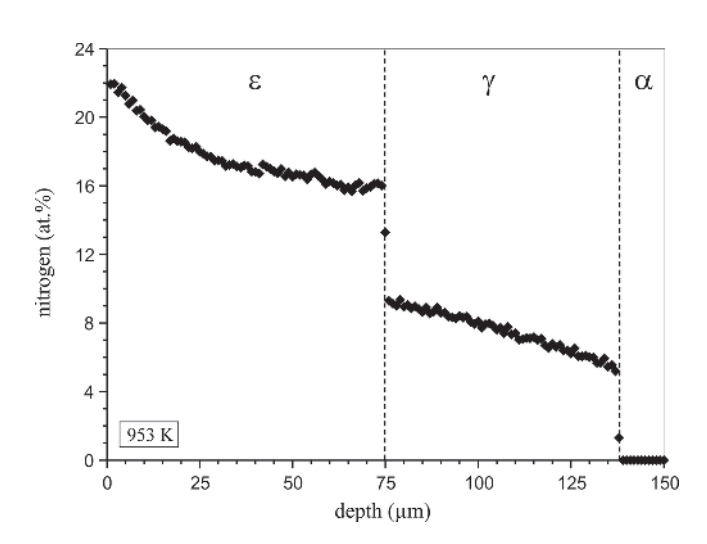


Fig. 2. Nitrogen concentration—depth profile determined by EPMA in an ε/γ double layer obtained upon nitriding at 953 K and $r_{\rm N}=0.5~{\rm atm^{-1/2}}$ (see Table 1). The dashed vertical lines indicate the ε/γ and γ/α interfaces.

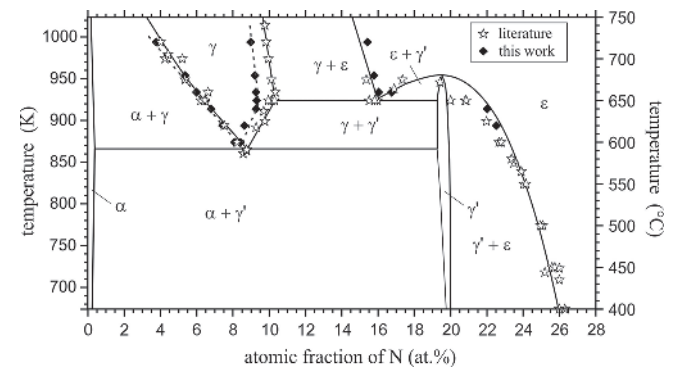
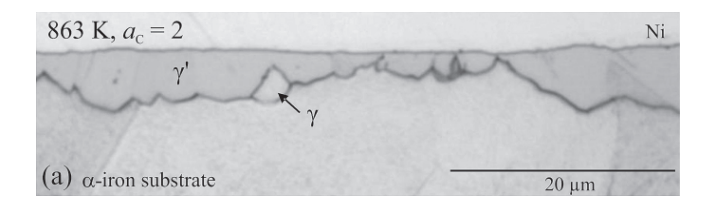


Fig. 3. Nitrogen contents (data points) in γ and ϵ at the corresponding phase boundaries determined by EPMA in compound layers of series N, superimposed on the binary Fe–N phase diagram (solid lines) [21] and experimental data cited there. The dashed lines indicate the homogeneity range of the γ phase according to the present work.

 $\theta/\epsilon/\gamma$ layer sequence. At 873 K the ϵ phase was nearly completely isolated from the α -iron substrate by a γ sublayer, i.e. a $\theta/\epsilon/\gamma$ layer was present. Only at very few places was the γ layer not closed. Note that for the specimens obtained at 868 K and 873 K, at a few places plates of θ phase from the θ sublayer extend through the ϵ sublayer to the α substrate (868 K) or to γ (873 K).



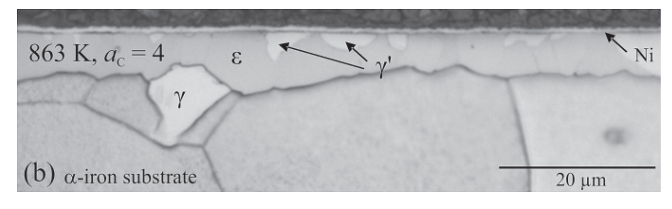
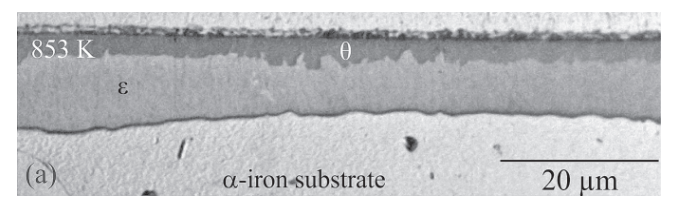
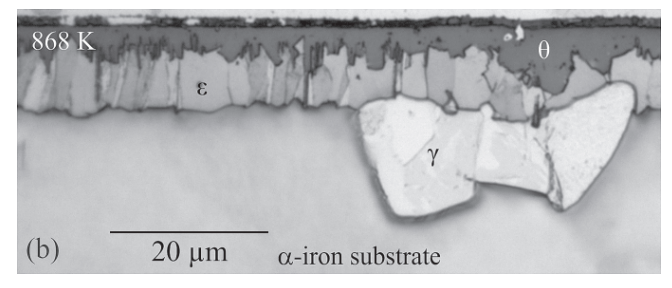


Fig. 4. Cross-sectional optical micrographs (after etching with 1 vol.% Nital containing 0.1 vol.% HCl) of the compound layers obtained upon nitrocarburising of a pure α -iron substrate for 4 h in gas mixture (series NC863) with $a_{\rm N}=109$ and (a) $a_{\rm C}=2$ and (b) $a_{\rm C}=4$ at 863 K.





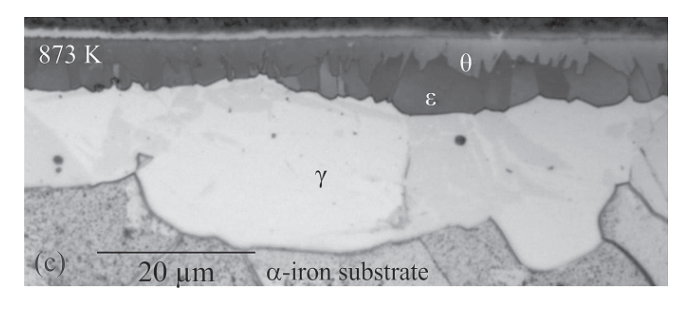
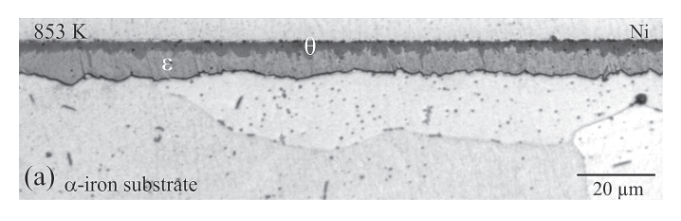


Fig. 5. Cross-sectional optical micrographs (after etching with 1 vol.% Nital containing 0.1 vol.% HCl and staining with Groesbeck reagent) showing cross-sections of the compound layers obtained upon nitrocarburising of presaturated α -iron substrates for 4 h in an NH $_3$ H $_2$ /CO/N $_2$ gas mixture (series NC) at (a) 853 K, (b) 868 K and (c) 873 K. The slight gap between the cementite (θ) sublayer at the surface of the specimen and the Ni capping layer is an artifact of the metallographic preparation.

The θ/ϵ double layer obtained upon nitrocarburising at 853 K (series NC; see Fig. 5a and Fig. 6a) was annealed for 24 h at a higher temperature of 873 K leading to a compound layer composed of a single-phase θ layer; at a few locations a θ/γ double layer was observed (Fig. 6b).

3.3. Nitrocarburising experiments of Series NC853 and NC893

The microstructure of compound layers obtained under the condition of nitrocarburising of series NC853 (Table 2) have already been discussed in Ref. [13]. Experiments of series NC853 with $a_{\rm N} = 553$ yielded ε/γ' double layers for $0 \le a_{\rm C} \le 50$ and an inhomogeneous microstructure com-



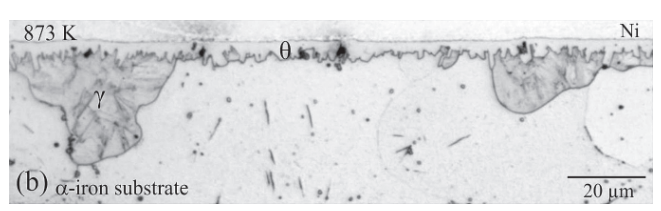
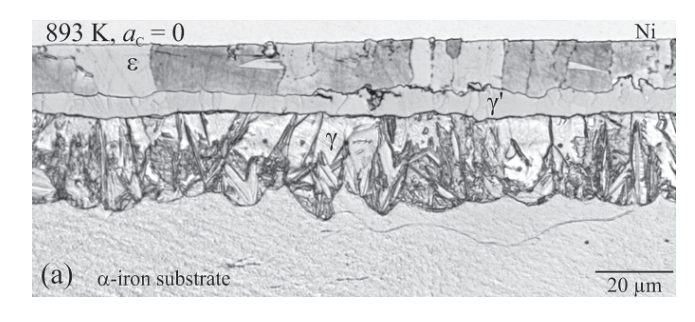


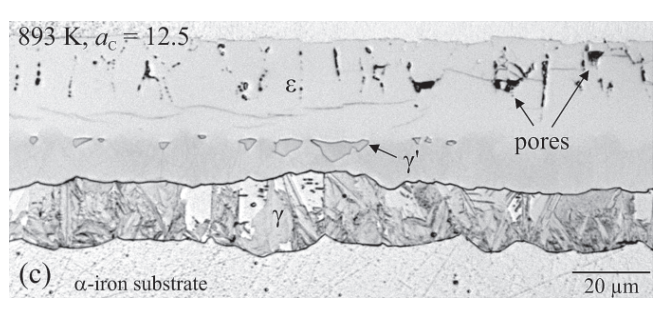
Fig. 6. Cross-sectional optical micrographs after etching with 1 vol.% Nital containing 0.1 vol.% HCl showing compound layers obtained after nitrocarburising (a) at 853 K, series NC (after staining with a Groesbeck reagent) and (b) after secondary annealing that specimen for 24 h at 873 K (no staining was applied).

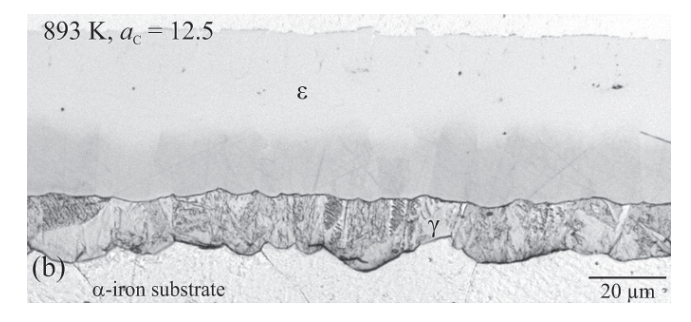
posed of both ε/γ' double layers and $\varepsilon/\varepsilon + \gamma'$ double layers for $100 \le a_{\rm C} \le 500$ [13]. Experiments of series NC853 with $a_{\rm N} = 416$ resulted in the formation of massive γ' layers for $0 \le a_{\rm C} \le 15$, ε/γ' double layers for $30 \le a_{\rm C} \le 100$ or inhomogeneous microstructures composed of both ε/γ' double layers and $\varepsilon/\varepsilon + \gamma'$ double layers for $200 \le a_{\rm C} \le 500$. Note that the γ phase was never observed in specimens nitrocarburized at 853 K.

Nitrocarburising experiments of series NC893 ($a_{\rm N}=626$) led to formation of $\varepsilon/\gamma'/\gamma$ layers (Fig. 7a) at carbon activities of $0 \le a_{\rm C} \le 1$. At higher carbon activities ($5 \le a_{\rm C} \le 25$), the amount of γ' in the compound layer decreases, leading to a laterally inhomogeneous microstructure of ε/γ layers (Fig. 7b) and $\varepsilon/\varepsilon + \gamma'/\varepsilon/\gamma$ layers (Fig. 7c). The occurrence of cementite was observed at $50 \le a_{\rm C} \le 200$; the corresponding microstructures were either laterally inhomogeneous, constituted of $\theta/\varepsilon/\gamma$ -layers and ε/γ layers, or homogeneous, i.e. $\theta/\varepsilon/\gamma$ layers were observed (Fig. 7d).

Representative nitrogen and carbon concentration-depth profiles determined in the ϵ and γ phases of compound layers obtained upon nitrocarburising of series NC853, NC893 as well as of series NC (at 853 K) are shown as data points in Fig. 8 and can be interpreted as part of the corresponding diffusion paths [2]. In specimens also exhibiting $\varepsilon + \gamma'$ dual-phase sublayers (e.g. Fig. 7c), the composition-depth profiles were only measured at locations, where the ε phase reaches from the surface to the ε/α interface, i. e. the γ' grains were avoided in the EPMA measurements. A composition–depth profile in the ε phase of a $\theta/\varepsilon/\gamma'$ layer (micrograph not shown) was also included in the isothermal section pertaining to 893 K in Fig. 8. The corresponding layer was obtained by first producing a massive γ' surface layer upon nitriding for 6 h at 853 K with 37.3 vol.% NH₃ and 62.7 vol.% H₂ and then nitrocarburising under the same conditions used for series NC.







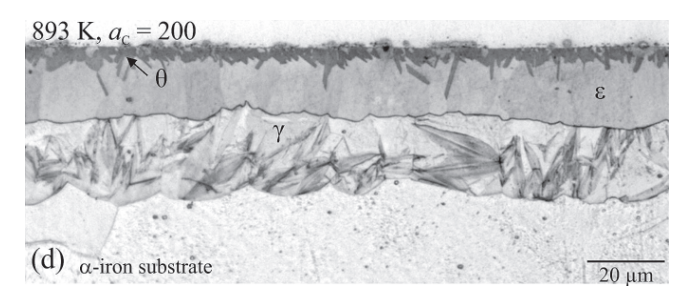


Fig. 7. Cross-sectional optical micrographs, after etching with 1 vol.% Nital containing 0.1 vol.% HCl and staining with a Groesbeck reagent, of compound layers obtained upon nitrocarburising of pure α -iron substrates for 4 h at 893 K (series NC893) using a nitrogen activity of $a_{\rm N}=626$ and a various carbon activities. (a) $\epsilon/\gamma'/\gamma$ layer, (b) ϵ/γ layer, (c) $\epsilon/\epsilon+\gamma'/\epsilon/\gamma$ layer, and (d) $\theta/\epsilon/\gamma$ layer. For $a_{\rm C}=12.5$ two micrographs taken from the same specimen are shown (b and c).

4. Discussion

198

The investigation of phase equilibria in the binary Fe-N and the ternary Fe-N-C system by means of nitriding/nitrocarburising of pure α -iron substrates is usually based on the assumption of local equilibrium at all solid-solid interphase boundaries in the developing compound layer. Under this assumption the mechanical contact of the phases in the compound layer obtained at a given process temperature implies the presence of corresponding phase equilibria in the corresponding Fe-N or Fe-N-C system. It turns out, however, that a few of the observed microstructures cannot be reconciled with the assumption of local equilibrium; see what follows in Section 4.2.2. Deviation from local equilibrium at solid-solid interfaces is in principle a well-established phenomenon [6]. In such cases a critical assessment of the experimental data is required to arrive at statements on the true equilibria. Note that the (possible) establishment of local equilibrium or stationary state [43] at the interface of the gas atmosphere and the compound layer is not relevant for the present work and is left undiscussed in the following.

4.1. The Fe-N system between 873 K and 993 K

Nitriding of pure α -iron substrates (Section 3.1, series N) in the range of 873 K–993 K resulted with increasing temperature in the formation of $\epsilon/\gamma'/\gamma$ layers, $\epsilon/\gamma'/\epsilon/\gamma$ layers and ϵ/γ double-layers, in that order. All these microstructures are compatible with the binary Fe–N phase diagram of Ref. [21].

The change of the microstructure from an $\epsilon/\gamma'/\gamma$ layer observed at 923 K to an $\epsilon/\gamma'/\epsilon/\gamma$ layer observed at 925 K implies the occurrence of the eutectoid transformation at a temperature between 923 K and 925 K (see Table 1), which is in very good agreement with the value of 923 K given in Ref. [21]. The disappearance of the γ' phase from the compound layers in the temperature range of 938 K–948 K implies that the temperature of the polymorphic transformation is in the range of 938 K–948 K. Thereby, the temperature of the polymorphic transformation is slightly lower than 953 K as indicated in the Fe–N phase diagram of Ref. [21]. It is noted that the temperatures of these invariant reactions in the binary Fe–N system are well reproduced by the different thermodynamic descriptions of the system [26–31].

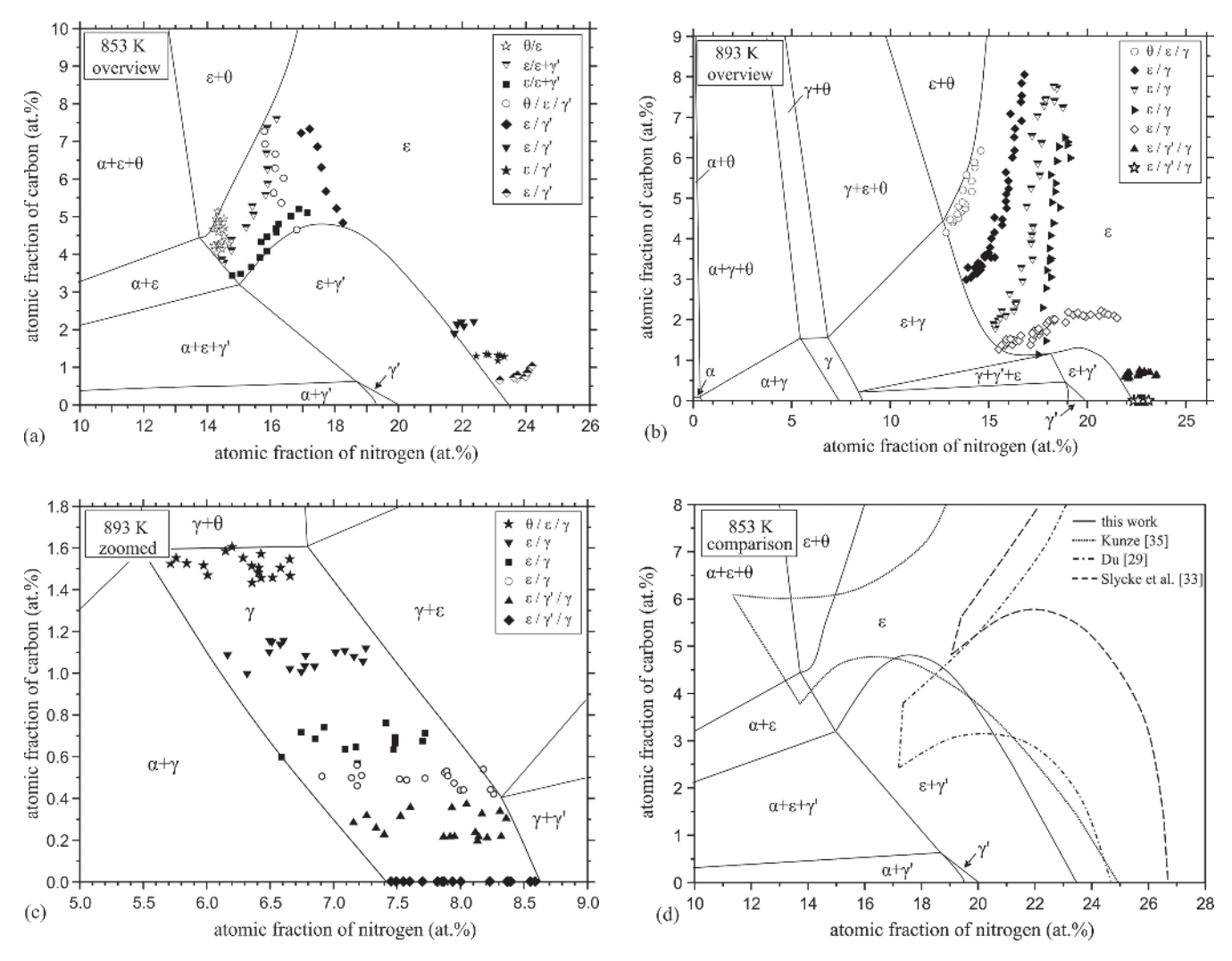


Fig. 8. Isothermal sections of the ternary Fe–N–C phase diagram at 1 atm superimposed with some of the diffusion paths measured in the compound layers obtained upon nitrocarburising at (a) 853 K as well as at (b) and (c) 893 K. The phase boundaries (full lines) were adapted to be compatible with the diffusion paths (points) in the ε and γ phase fields measured by EPMA (individual, unaveraged profiles). The legend indicates the layer sequences observed for the specimens, in which the EPMA profiles were taken. (d) Comparison of the presently assessed phase boundaries at 853 K with the extent of the ε phase field as reported by previous authors [29, 33, 35].

The nitrogen contents in ε as determined by EPMA at the $\varepsilon/\varepsilon + \gamma'$ phase boundary and the $\varepsilon/\varepsilon + \gamma$ phase boundary agree well with the Fe-N phase diagram of Ref. [21] (see Fig. 3); the deviations are less than 0.4 at.% N. Also the γ / $\gamma + \alpha$ phase boundary excellently agrees with literature data [51–55]. However, the nitrogen contents at the $\gamma/\gamma + \gamma'$ and the $\gamma/\gamma + \varepsilon$ phase boundaries obtained in the present work are up to 1 at.% lower than the values given in Refs. [51– 55]; see Fig. 3. Therefore, the numerical values have been added to Table 1. The agreement of the presently determined low-N content phase boundary of the γ phase with the literature [21] implies that the disagreement of the high-N content phase boundaries of the γ phase cannot be simply attributed to some possible systematic error in the N-content determination by EPMA as performed in this work.

4.2. The Fe-N-C system between 853 K and 893 K

4.2.1. General

The results of the nitrocarburising and of the secondary annealing experiments in terms of phase boundaries and in terms of occurrence of different solid state equilibria were used to construct isothermal sections at 853 K and at 893 K, as shown in Fig. 8. The experimental results also indicate that two invariant reactions occur in this temperature range. A eutectoid reaction $\gamma \rightleftharpoons \alpha + \gamma' + \varepsilon$ at a single temperature in the range of 853 K < $T_{\rm E}$ < 863 K and a transition reaction $\gamma + \theta \rightleftharpoons \alpha + \varepsilon$ at a single temperature in the range of 868 K < $T_{\rm U2}^2$ < 873 K. The corresponding four-phase equilibria prevailing at the respective invariant temperatures are illustrated in Fig. 9. The invariant reactions are also indicated in the Scheil reaction scheme [56, 57] shown in Fig. 10, where the invariant reactions for the two binary systems have been obtained from the literature [21, 58].

These two invariant reactions are both predicted to occur by three different descriptions of the Fe–N–C system [29, 32, 35]. Therefore, the following discussion focusses at a comparison of the present experimental results with these thermodynamic descriptions. Note that the sequence of invariant reactions reported on the basis of a very recent thermodynamic description [37] is different from those in [29, 32, 35]. Moreover, according to Ref. [37] the $\gamma + \theta$ equilibrium would occur above 848 K, above which also the $\alpha + \epsilon$ equilibrium would be absent.

4.2.2. Temperatures of the invariant reactions

The temperature range indicated for the invariant temperature $T_{\rm E}$ is determined as follows. The microstructures of series NC863 reveal that the γ phase was formed in the compound layer upon nitrocarburising at 863 K (series NC863; see Section 3.2 and Fig. 4), whereas this was not the case at 853 K (series NC853, Section 3.3, and numerous, not mentioned, experiments performed at this temperature, see [13, 14, 40]). Non-observation of the γ phase in the large variety of microstructures obtained at 853 K contain-

ing α , γ' and ε , indicates that the invariant reaction $\gamma \rightleftharpoons \alpha + \gamma' + \varepsilon$ occurs within the above indicated 853 K < $T_{\rm E}$ < 863 K. A comparison with the binary Fe–N phase diagram (Fig. 3), where the invariant reaction $\gamma \rightleftharpoons \alpha + \gamma'$ occurs at 865 K shows that the eutectoid temperature pertaining to the ternary system is, as expected, lower than for the binary Fe–N system.

The temperature range indicated for the invariant temperature $T_{\rm II2}$ is determined on the basis of the observations of the specimens of series NC using presaturated substrates, as well as on observations of specimens subjected to secondary annealing. The treatment conditions of series NC were chosen such that the θ phase forms at the surface of the compound layer, in agreement with Refs. [15, 41]. The obtained microstructures at the interface with the α substrate indicate the presence of the two-phase equilibrium α + ε at 853 K – 868 K whereas at 873 K an α + γ two-phase equilibrium occurs at most places (Fig. 5). However, for a treatment temperature of 868 K a few θ platelets penetrating the ε sublayer are in direct contact with the γ -phase regions, although a $\gamma + \theta$ equilibrium does not exist at that temperature (only above T_{U2}). Similarly, for a treatment temperature of 873 K, at a very few places, the γ phase is not fully closed and a few ε grains are in contact with the α substrate, although an α + ϵ equilibrium does not exist at that temperature (only below $T_{\rm U2}$). These observations imply that non-equilibrium states may also be encountered. The chosen value of T_{U2} of 868 K < T_{U2} < 873 K is also compatible with secondary annealing of the specimen nitrocarburized at 853 K of the NC series at a higher temperature of 873 K which resulted in the disappearance of the $\varepsilon + \alpha$ equilibrium and the establishment of the $\gamma + \theta$ equilibrium in the microstructure of the compound layer (Fig. 6).

The eutectoid reaction $\gamma \rightleftharpoons \alpha + \gamma' + \varepsilon$ (invariant temperature $T_{\rm E}$) and the transition reaction $\gamma + \theta \rightleftharpoons \alpha + \varepsilon$ (invariant temperature T_{U2}) have been predicted by various thermodynamic descriptions of the Fe-N-C system [29, 32, 35]. In the case of the eutectoid reaction, it has been reported $T_E = 849 \text{ K}$ by Du and Hillert [32], 856 K by Du [29], and 856 K by Kunze³ [35], which should be compared with 853 K-863 K as found here experimentally. In the case of the transition reaction, it has been reported $T_{\rm U2}$ = 853 K by Du and Hillert [32], 867 K by Du [29], and 951 K by Kunze³ [35]. These values have to be compared with $T_{\rm U2} = 868 \text{ K} - 873 \text{ K}$ as found here experimentally. Hence, considering *only* the values of the invariant temperatures, the thermodynamic description by Du [29] agrees best with the presently reported experimental data (but see Section 4.2.3).

In a recent work [59] the presence of a pearlite-like microstructure in compound layers of carbon steel nitrocarburized at 833 K-853 K followed by furnace cooling was observed. That microstructure was attributed to the presence of nitrogen-rich austenite at the treatment temperature, which was reconciled with outdated constitution data of the Fe–N–C system [25] in which a eutectoid temperature of as low as 838 K (or below) was proposed. Such a low value of $T_{\rm E}$, however, has to be rejected in view of the later literature and also in view of the present work, and casts doubts on the temperature control of the experiments

² This transition temperature is associated with the index 2 to distinguish this transition temperature from the temperature of a second transition reaction $\alpha + \epsilon \rightleftharpoons \theta + \gamma'$ reported to occur at a lower temperature, in the range 833 K-843 K [38].

³ These values have not been reported in Ref. [35] but have been calculated separately in this work.

presented in [59]. The present authors have never observed signs of austenite in specimens nitrocarburised at 853 K.

4.2.3. Extent of the ε -phase field

Whereas early works [23–25, 36] implied the absence of an $\alpha + \epsilon$ equilibrium in the ternary Fe–N–C system, some experimental evidence (see references listed in Ref. [38]) indicated occurrence of that equilibrium. In fact, later reported thermodynamic descriptions [29, 32–35] of the Fe–N–C system imply the presence of a corresponding $\alpha + \epsilon$ two-phase field at 853 K. Quite direct experimental evidence was obtained with later data [38]. Hence, the presence of the $\alpha + \epsilon$ two-phase field in the isothermal section at 853 K (Fig. 8) is compatible with the recent literature. The isothermal sections calculated from the thermodynamic descriptions by Du and Hillert [32], Du [29], Kunze [35] and Slycke et al. [33] for a temperature of 853 K do

all contain an $\alpha + \epsilon$ two-phase region. A comparison of the calculated [29, 33, 35] and the experimentally determined Fe–N–C phase diagram isothermal sections at 853 K is given in Fig. 8d. Evidently, the thermodynamic description according to Kunze [35] shows the best but still limited agreement with the experimental data.

5. Conclusion

New experimental data on phase boundaries and invariant reactions have been determined for the (metastable) Fe–N and Fe–N–C systems. For that purpose, compound layers composed of iron (carbo)nitrides and partly cementite were generated by means of gaseous nitriding or nitrocarburising on α -iron plates or α -iron plates pre-saturated with nitrogen. In some cases, specimens were subsequently annealed in an inert atmosphere. In most cases the microstructures were evaluated by interpreting phases in contact with each other

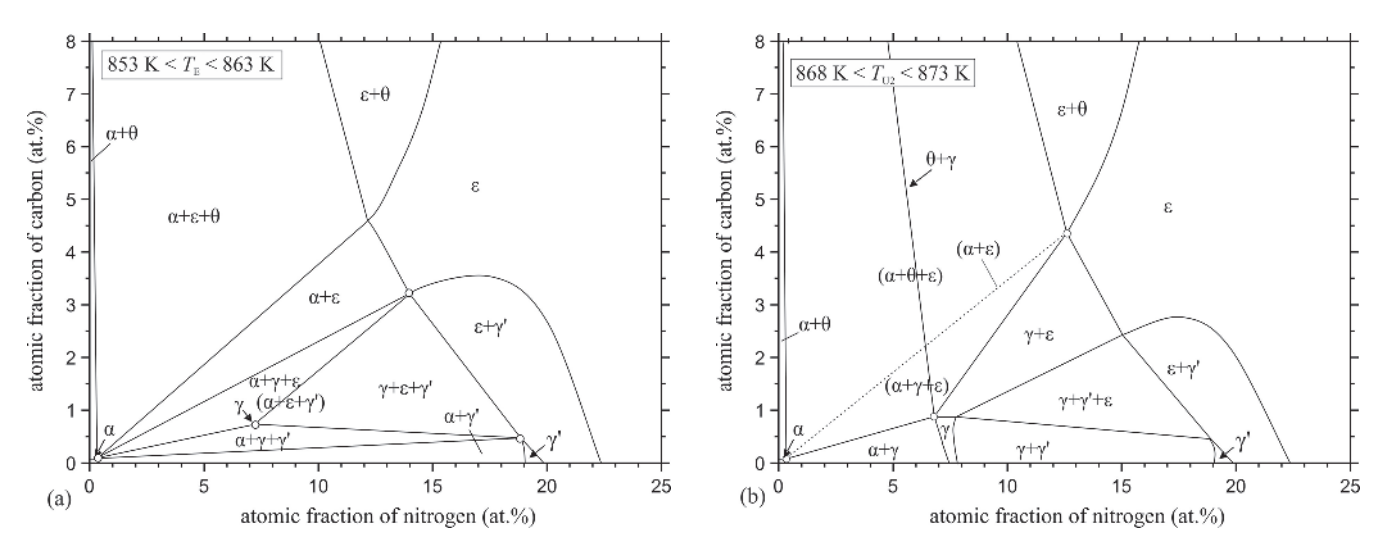


Fig. 9. Invariant four-phase equilibria represented by the ternary Fe–N–C phase diagram at 1 atm immediately *above* the corresponding invariant temperature (a) $\gamma \rightleftharpoons \alpha + \gamma' + \epsilon$ (853 K < $T_{\rm E}$ < 863 K) and (b) $\gamma + \theta \rightleftharpoons \alpha + \epsilon$ (868 K < $T_{\rm U2}$ < 873 K). In line with Ref. [57] the compositions of the four phases participating at the corresponding equilibrium have been indicated by circles, whereby the composition of the cementite θ (25 at. % C) contributing to the four-phase equilibrium in (b) is not located in the range shown. The two-phase and three-phase equilibria occurring immediately *below* the invariant temperature have been labelled with the phase identifiers in parentheses. Thereby, the new two-phase equilibrium appearing below the invariant transition temperature in (b) has been indicated by a dashed line.

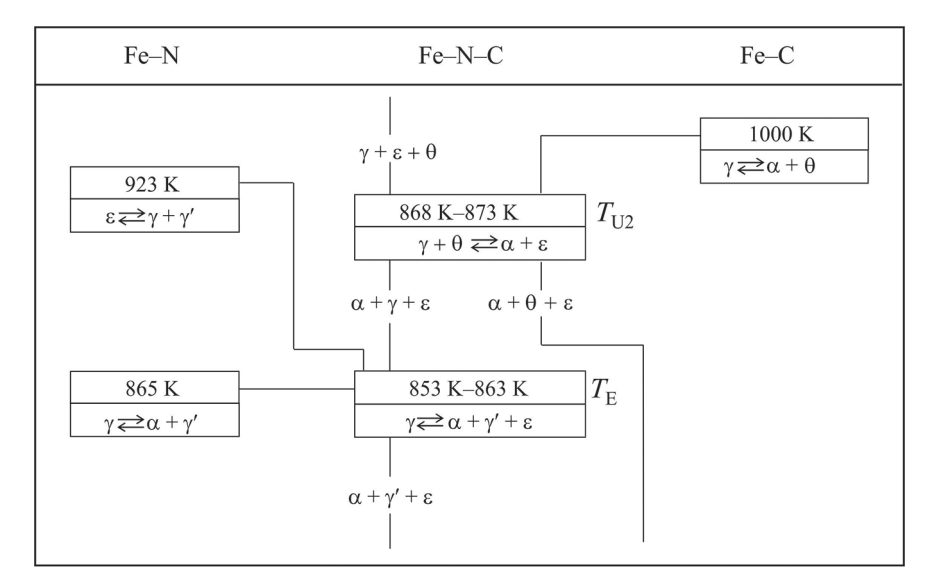


Fig. 10. Part of the Scheil reaction scheme of the metastable Fe–N–C system showing the sequence, formula and temperature of the invariant and univariant reactions for the ternary Fe–N–C system at 1 atm as obtained in the present work, i.e. reactions occurring below the ternary eutectoid are not considered. The lines connecting the invariant reactions represent the corresponding three-phase equilibria. For the binary Fe–N and Fe–C systems, the data were taken from the literature [21, 58].

as to be in (local) equilibrium at the nitriding/nitrocarburising temperature or, in the case of annealed specimens, at the last applied annealing temperature. For a few specimens, however, the presence of a non-equilibrium microstructure had to be assumed to arrive at a definite view on the equilibrium phase diagram. Electron microprobe analysis measurements were employed to determine the homogeneity ranges of the ϵ and γ phase fields. The following conclusions were drawn:

- 1. The microstructures of compound layers of α -iron plates purely *nitrided* at 873 K 993 K largely agree well with what is expected from published Fe–N phase diagrams. However, the phase boundaries $\gamma/\gamma + \gamma'$ and $\gamma/\gamma + \epsilon$ are shifted distinctly to lower N contents by about 1 at.%.
- 2. In the Fe–N–C system two invariant reactions occur in the temperature range 853 K–893 K as demonstrated on the basis of microstructures of compound layers of as-nitrocarburised α-iron plates, and those of some specimens which were subsequently subjected to further anneals: the eutectoid reaction, γ = α + γ' + ε, occurs in the range 853 K–863 K, and the transition reaction, γ + θ = α + ε, occurs in the range 868 K–873 K. Isothermal sections of the Fe–N–C system at 853 K and 893 K can be constructed from these data and the concentration–depth profiles in the ε and γ phases.
- 3. A comparison has been made of the obtained constitutional data for the Fe-N-C system with those calculated, by means of the Calphad method, on the basis of different thermodynamic descriptions of the Fe-N-C system reported in the literature. Such a comparison shows that the description by Kunze [35] gives the best agreement regarding the composition ranges of the ε phase, whereas the description by Du [29] agrees best regarding the temperatures of the invariant reactions considered here. It can be concluded here that an improved thermodynamic description of the Fe-N-C system might be found as a compromise of the models of Refs. [29, 35]. Such an improved description is relevant due to occurrence of several invariant reactions in the Fe-N-C system within the temperature range of technical nitriding and nitrocarburising procedures (typically below the eutectoid temperature) and slightly above.

We thank Dipl.-Ing. Holger Göhring for calculation, using the Thermo-Calc software, of the invariant temperatures on the basis of Kunze's thermodynamic description [35]. These values were not provided in the original work.

References

- [1] J.S. Kirkaldy, D.J. Young: Diffusion in the Condensated State, The Institute of Metals, London (1987).
- [2] A.A. Kodentsov, G.F. Bastin, F.J.J. Van Loo: J. Alloys Compd. 320 (2001) 207. DOI:10.1016/S0925-8388(00)01487-0
- [3] F.J.J. Van Loo: Progr. Solid State Chem. 20 (1990) 47. DOI:10.1016/0079-6786(90)90007-3
- [4] F.J.J. Van Loo, M.R. Rijnders, K.J. Ronka, J.H. Gulpen, A.A. Kodentsov: Solid State Ionics 95 (1997) 95. DOI:10.1016/S0167-2738(96)00550-4
- [5] N.H. Christensen: J. Am. Ceram. Soc 60 (1977) 293. DOI:10.1111/j.1151-2916.1977.tb15544.x
- [6] U. Gösele, K.N. Tu: J. Appl. Phys. 53 (1982) 3252. DOI:10.1063/1.331028
- [7] E.J. Mittemeijer in: J.I. Dosset, G.E. Totten (Eds.), Fundamentals of Nitriding and Nitrocarburizing, ASM Handbook, Vol. 4A (2013) 619.

- [8] E.J. Mittemeijer, M.A.J. Somers: Surf. Eng. 13 (1997) 483. DOI:10.1179/sur.1997.13.6.483
- [9] M.A.J. Somers: Heat Treat. Met. 4 (2000) 92.
- [10] P.F. Colijn, E.J. Mittemeijer, H.C.F. Rozendaal: Z. Metallkd. 74 (1983) 620.
- [11] J. Slycke, L. Sproge: Surf. Eng. 5 (1989) 125.DOI:10.1179/sur.1989.5.2.125
- [12] W.-D. Jentzsch, S. Böhmer: Krist. Techn. 14 (1979) 617. DOI:10.1002/crat.19790140516
- [13] T. Woehrle, A. Leineweber, E.J. Mittemeijer: HTM J. Heat Treat. Mater. 65 (2010) 243. DOI:10.3139/105.110069
- [14] T. Woehrle, A. Leineweber, E.J. Mittemeijer: Metall. Mater. Trans A 44 (2013) 2548. DOI:10.1007/s11661-013-1640-z
- [15] T. Gressmann, M. Nikolussi, A. Leineweber, E.J. Mittemeijer: Scr. Mater. 55 (2006) 723. DOI:10.1016/j.scriptamat.2006.06.022
- [16] M.A.J. Somers, E.J. Mittemeijer: Surf. Eng. 3 (1987) 123. DOI:10.1179/sur.1987.3.2.123
- [17] H. Du, M.A.J. Somers, J. Ågren: Metall. Mater. Trans. A 31 (2000) 195. DOI:10.1007/s11661-000-0065-7
- [18] T. Bell: Heat Treat. Met. 2 (1975) 39.
- [19] C. Dawes, D.F. Tranter: Heat Treat. Met. 3 (1985) 70.
- [20] E.J. Mittemeijer: J. Heat Treat. 3 (1983) 114. DOI:10.1007/BF02833081
- [21] H.A. Wriedt, N.A. Gokcen, R.H. Nafziger: Bull. Alloy Phase Diagr. 8 (1987) 355. DOI:10.1007/BF02869273
- [22] K.H. Jack: Proc. Roy. Soc. London A 208 (1951) 200. DOI:10.1098/rspa.1951.0154
- [23] V. Raghavan: Trans. Ind. Inst. Met. 37 (1984) 293.
- [24] V. Raghavan: J. Phase Equilib. 14 (1993) 620. DOI:10.1007/BF02669146
- [25] F.K. Naumann, G. Langenscheid: Archiv Eisenhüttenwesen 8 (1965) 583.
- [26] K. Frisk: CALPHAD 11 (1987) 127. DOI:10.1016/0364-5916(87)90004-6
- [27] M. Hillert, M. Jarl: Metall. Trans. A 6 (1975) 553. DOI:10.1007/BF02658414
- [28] J. Kunze: Steel Res. 57 (1986) 361.
- [29] H. Du: J. Phase Equilib. 14 (1993) 682. DOI:10.1007/BF02667880
- [30] H. Du, A. Fernández Guillermet: Z. Metallkd. 85 (1994) 154.
- [31] B.J. Kooi, M.A.J. Somers, E.J. Mittemeijer: Metall. Mater. Trans. A 27 (1996) 1063. DOI:10.1007/BF02649775
- [32] H. Du, M. Hillert: Z. Metallkd. 82 (1991) 310.
- [33] J. Slycke, L. Sproge, J. Ågren: Scand. J. Metall. 17 (1988) 122.
- [34] J. Kunze: Nitrogen and Carbon in Iron and Steel, Akademie-Verlag, Berlin (1990).
- [35] J. Kunze: HTM Härterei Tech. Mit. 51 (1996) 348.
- [36] X. Zuyoa, L. Lin: Mat. Sci. Technol. 3 (1987) 325. DOI:10.1179/mst.1987.3.5.325
- [37] P. Franke, H.J. Seifert (Eds.): Thermodynamic Properties of Inorganic Materials compiled by SGTE, Subvolume C, Part 1 Landolt-Börnstein, Numerical Data and Functional Relationships in Science and Technology, new Series, Group IV: Physical Chemistry, Volume 19C1 (2012) p. 183–188.
- [38] M. Nikolussi, A. Leineweber, E. Bischoff, E.J. Mittemeijer: Int. J. Mater. Res. 98 (2007) 1086. DOI:10.3139/146.101576
- [39] A. Leineweber, T. Liapina, T. Gressmann, M. Nikolussi, E.J. Mittemeijer: Adv. Sci. Technol. 46 (2006) 32. DOI:10.4028/www.scientific.net/AST.46.32
- [40] T. Woehrle, A. Leineweber, E.J. Mittemeijer: Metall. Mater. Trans. A 43 (2012) 2401. DOI:10.1007/s11661-012-1100-1
- [41] M. Nikolussi, A. Leineweber, E.J. Mittemeijer: Philos. Mag. 90 (2010) 1105. DOI:10.1080/14786430903292365
- [42] T. Liapina, A. Leineweber, E.J. Mittemeijer: Metall. Mater. Trans. A 37 (2006) 319. DOI:10.1007/s11661-006-0003-4
- [43] J. Stein, R.E. Schacherl, M. Jung, S. Meka, B. Rheingans, E.J. Mittemeijer: Int. J. Mater. Res. 104 (2013) 1053. DOI:10.3139/146.110968
- [44] R. Hoffmann, E.J. Mittemeijer, M.A.J. Somers: HTM Härterei Tech. Mit. 51 (1996) 162.
- [45] E. Lehrer: Z. Elektrochem. 36 (1930) 383.
- [46] A. Leineweber, T. Gressmann, E.J. Mittemeijer: Surf. Coat. Technol. 206 (2012) 2780. DOI:10.1016/j.surfcoat.2011.11.035
- [47] M. Nikolussi, A. Leineweber, E.J. Mittemeijer: J. Mater. Sci. 44 (2009) 770. DOI:10.1007/s10853-008-3160-6

- [48] A. Wells: J. Mater. Sci. 20 (1985) 2439. DOI:10.1007/BF00556072
- [49] G. Petzow: Metallographic Etching, ASM International, Ohio, USA (1999).
- [50] J.L. Pochau, F. Pichoir: Rech. Aerospatial 3 (1983) 167.
 [51] E. Scheil, W. Mayr, J. Müller: Archiv Eisenhüttenwesen 33 (1962) 385.
- [52] O. Eisenhut, E. Kaupp: Z. Elektrochem. 36 (1930) 392.
- [53] E. Lehrer: Z. Elektrochem. 36 (1930) 460.
- [54] V.G. Paranjpe, M. Cohen, M.B. Bever, C.F. Floe: Trans. AIME 188 (1950) 261.
- [55] D. Atkinson, C. Bodsworth: J. Iron Steel Int. 208 (1970) 587.
- [56] H.L. Lukas, E.T. Henig, G. Petzow: Z. Metallkd. 77 (1986) 360.
 [57] B. Predel, M. Hoch, M.J. Pool: Phase Diagrams and Heterogeneous Equilibria, Springer, Berlin, Heidelberg (2004). DOI:10.1007/978-3-662-09276-7
- [58] J. Chipman: Metall. Trans. 3 (1972) 55. DOI:10.1007/BF02680585
- [59] W.L. Chen, C.L. Wu, Z.R. Liu, S. Ni, Y. Hong, Y. Zhang, J.H. Chen: Acta Mater. 61 (2013) 3963. DOI:10.1016/j.actamat.2013.02.058

(Received September 8, 2015; accepted November 23, 2015; online since January 7, 2016)

Correspondence address

Prof. Dr. Andreas Leineweber Institute of Materials Science TU Bergakademie Freiberg Gustav-Zeuner-Straße 5 09599 Freiberg Germany Tel.: +49 3731 39-2622

E-mail: andreas.leineweber@iww.tu-freiberg.de

Bibliography

DOI 10.3139/146.111341 Int. J. Mater. Res. (formerly Z. Metallkd.) 107 (2016) 3; page 192–202 © Carl Hanser Verlag GmbH & Co. KG ISSN 1862-5282